



The Effect of Temperature Dependent Material Nonlinearities on the Response of Piezoelectric Composite Plates

Ho-Jun Lee
Lewis Research Center, Cleveland, Ohio

Dimitris A. Saravanos
Ohio Aerospace Institute, Brook Park, Ohio

National Aeronautics and
Space Administration

Lewis Research Center

Available from

NASA Center for Aerospace Information
800 Elkridge Landing Road
Linthicum Heights, MD 21090-2934
Price Code: A03

National Technical Information Service
5287 Port Royal Road
Springfield, VA 22100
Price Code: A03

THE EFFECT OF TEMPERATURE DEPENDENT MATERIAL NONLINEARITIES ON THE RESPONSE OF PIEZOELECTRIC COMPOSITE PLATES

Ho-Jun Lee
National Aeronautics and Space Administration
Lewis Research Center
Cleveland, Ohio 44135

and

Dimitris A. Saravanos*
Ohio Aerospace Institute
Brook Park, Ohio 44142

ABSTRACT

Previously developed analytical formulations for piezoelectric composite plates are extended to account for the nonlinear effects of temperature on material properties. The temperature dependence of the composite and piezoelectric properties are represented at the material level through the thermopiezoelectric constitutive equations. In addition to capturing thermal effects from temperature dependent material properties, this formulation also accounts for thermal effects arising from: (1) coefficient of thermal expansion mismatch between the various composite and piezoelectric plies and (2) pyroelectric effects on the piezoelectric material. The constitutive equations are incorporated into a layerwise laminate theory to provide a unified representation of the coupled mechanical, electrical, and thermal behavior of smart structures. Corresponding finite element equations are derived and implemented for a bilinear plate element with the inherent capability to model both the active and sensory response of piezoelectric composite laminates. Numerical studies are conducted on a simply supported composite plate with attached piezoceramic patches under thermal gradients to investigate the nonlinear effects of material property temperature dependence on the displacements, sensory voltages, active voltages required to minimize thermal deflections, and the resultant stress states.

NOMENCLATURE

a	: length of plate	F_{th}	: thermal force vector
b	: width of plate	h	: thickness of plate
D	: electric displacement	K	: stiffness matrix
d	: piezoelectric charge constant	M	: mass matrix
E	: electric field	p	: pyroelectric constant
F	: mechanical force vector	Q	: electric charge vector
f	: body force per unit volume	q	: surface electric charge

* NASA Resident Research Associate at Lewis Research Center

Q_{th}	: thermal electric charge vector
R	: in-plane shape functions
S	: strain
s	: elastic compliance
T	: temperature
t	: surface traction
U	: displacement state variable
u	: displacement
x,y,z	: structural axes
α	: coefficient of thermal expansion
ϵ	: electric permittivity
θ	: temperature difference
ρ	: mass density
σ	: stress
Φ	: electric potential state variable
ϕ	: electric potential
ψ	: through the thickness shape functions

Subscripts

$(, i)$: $\partial() / \partial u_i$
uu	: structural component
$u\phi, \phi u$: piezoelectric component
$\phi\phi$: dielectric component

Superscripts

$(\cdot\cdot)$: $\partial^2() / \partial t^2$
a	: active component
E	: constant voltage condition
s	: sensory component
T	: constant temperature condition
σ	: constant stress condition

INTRODUCTION

The development of structural components consisting of piezoelectric materials offers great potential for improving the performance of advanced aerospace vehicles. By taking advantage of the direct and converse piezoelectric effects, as well as the pyroelectric phenomena, piezoelectric composite materials can be utilized in a variety of shape, vibration, and noise control applications. These potential performance advantages have resulted in extensive development of both analytical and experimental methods to characterize the behavior of piezoelectric materials. Detailed overviews of the current state of piezoelectric material technology have been reported by Crawley (1994) and Rao and Sunar (1994).

Although the typical application of most aerospace structures will involve operations in extreme temperature environments, only limited research has been performed to study the implications of thermal effects on the active and sensory response of piezoelectric composite materials. In general, there are three distinct physical mechanisms which will influence the thermal response of piezoelectric composite structures: (1) induction of thermal stresses due to coefficient of thermal expansion (CTE) mismatch between the various composite and piezoelectric layers, (2) pyroelectric effects on the piezoelectric element, and (3) the temperature dependence of the composite and piezoelectric material properties. Previously reported analytical models incorporating thermal effects have investigated only the first two thermal physical mechanisms (i.e. CTE mismatch and pyroelectric phenomena). Mindlin (1974) initiated analytical studies of thermopiezoelectricity by formulating two-dimensional plate equations. Laminated thermopiezoelectric plate and thin shell theories were reported by Tauchert (1992) and Tzou and Howard (1994), respectively. Subsequent developments in thermopiezoelectric finite elements were performed by Rao and Sunar (1993), Jonnalagadda et al. (1994), Tzou and Ye (1994), and Chandrashekara and Kolli (1995). Many of these previous approaches utilize various single layer theories, which have been shown by Robbins and Reddy (1991, 1993) to have limitations in the analysis of both thick laminates and laminates

containing strong inhomogeneities. In order to remedy these limitations, layerwise thermopiezoelectric finite element approaches have been developed by Lee and Saravanos (1995, 1996a, 1996b).

This paper extends previously developed layerwise finite element formulations [Lee and Saravanos (1995, 1996a, 1996b)] to also account for the nonlinear temperature dependence of material properties. The updated mechanics provides a comprehensive thermal analysis capability for modeling smart structures, which captures the coupled mechanical, electrical, and thermal response of piezoelectric laminates at the material level through the thermopiezoelectric constitutive equations. A layerwise laminate theory is implemented with the displacements, electric potential, and temperature modeled as variable fields through the thickness to provide more accurate analysis of piezoelectric composite laminates. A corresponding finite element formulation is implemented for a bilinear plate element. Numerical studies are conducted to determine the nonlinear effects of incorporating material property temperature dependence on the displacements, sensory voltages, active voltages required to minimize the thermal deflections, and stresses of piezoelectric composite plates subject to thermal gradients.

GOVERNING EQUATIONS

This section outlines the governing equations required to develop the layerwise finite element formulation for thermopiezoelectric composite structures. The mechanical response is governed by the equations of motion

$$\sigma_{ij,j} + f_i = \rho \ddot{u}_i \quad (1)$$

while the electrical response is described by the electrostatic equation

$$D_{i,i} = 0 \quad (2)$$

where $i, j = 1, 2, 3$. The constitutive equations for a thermopiezoelectric material, with temperature dependent properties, employing standard contracted notation are

$$S_\alpha = s_{\alpha\beta}^{E,T}(T) \sigma_\beta + d_{\alpha m}^T(T) E_m + \alpha_\alpha^{E,T}(T) \theta \quad (3)$$

$$D_m = d_{m\alpha}^T(T) \sigma_\alpha + \epsilon_{mk}^{o,T}(T) E_k + p_m^{o,T}(T) \theta \quad (4)$$

where $\alpha, \beta = 1, \dots, 6$ and $k, m = 1, 2, 3$. The small deformation strain-displacement relations are

$$S_{ij} = \frac{1}{2} (u_{i,j} + u_{j,i}) \quad (5)$$

and the electric field vector is related to the electric potential by

$$E_i = - \phi_{,i} \quad (6)$$

Through use of the divergence theorem and neglecting body forces, Eqs. (1) and (2) can be expressed in an equivalent variational form as

$$\int_V (\rho \ddot{u}_i \delta u_i + \sigma_{ij} \delta S_{ij} - D_i \delta E_i) dV = \int_{\Gamma_t} t_i \delta u_i d\Gamma + \int_{\Gamma_p} q \delta \phi d\Gamma \quad (7)$$

where V represents the volume of both the composite and piezoelectric materials, Γ_t is the bounding surface on which surface tractions are applied, and Γ_p represents the piezoelectric material surface to which electrical charges are applied.

By incorporating Eqs. (3)-(6) and introducing both the layerwise and finite element approximations into Eq. (7), the following discretized finite element equations can be obtained in a compact form with the electrical potential partitioned into active and sensory components

$$\begin{bmatrix} [M_{uu}] & 0 \\ 0 & 0 \end{bmatrix} \begin{Bmatrix} \{\ddot{U}\} \\ \{\ddot{\Phi}^s\} \end{Bmatrix} + \begin{bmatrix} [K_{uu}] & [K_{u\phi}^{ss}] \\ [K_{\phi u}^{ss}] & [K_{\phi\phi}^{ss}] \end{bmatrix} \begin{Bmatrix} \{U\} \\ \{\Phi^s\} \end{Bmatrix} = \begin{Bmatrix} \{F\} + \{F_{th}\} - [K_{u\phi}^{sa}]\{\Phi^a\} \\ \{Q^s\} + \{Q_{th}^s\} - [K_{\phi\phi}^{sa}]\{\Phi^a\} \end{Bmatrix} \quad (8)$$

The mass, stiffness, external force, and thermal force submatrices are functions of the various material properties, interpolation functions, and plate geometric parameters such that

$$\begin{aligned} M_{uu} &= M_{uu}(\rho, \psi, R, a, b, h) \\ K_{uu} &= K_{uu}(C, \psi, R, a, b, h) \\ K_{u\phi} &= K_{u\phi}(e, \psi, R, a, b, h) \\ K_{\phi\phi} &= K_{\phi\phi}(\epsilon, \psi, R, a, b, h) \\ F_{th} &= F_{th}(\lambda, \psi, R, a, b, h) \\ Q_{th} &= Q_{th}(p, \psi, R, a, b, h) \end{aligned} \quad (9)$$

More detailed descriptions of the layerwise theory and finite element formulation, along with the specific forms of the submatrices can be found in Lee and Saravanos (1996b).

TEMPERATURE DEPENDENT MATERIAL PROPERTIES

The various elastic, dielectric, piezoelectric, and pyroelectric properties of piezoelectric materials are influenced differently by temperature variations depending on the composition and manufacturing technique. Piezoelectric materials also possess a characteristic limiting temperature, called the Curie temperature, beyond which the material loses its piezoelectric properties. Thus, in typical applications the operating temperatures must be considerably lower than the Curie temperature. In this study, temperature dependent material properties of a PZT-5A piezoceramic were obtained from manufacturer's data, while published properties of an AS4/3501-6 carbon/epoxy composite were acquired from Daniel and Ishai (1994).

The temperature variation of the piezoelectric and composite material properties are implemented into the constitutive equations Eqs. (3)-(4) in a piecewise linear fashion. The variation of PZT-5A properties (d_{31} , ϵ_{33} , α_{11} , and p_3) are shown in Figure 1, while the temperature dependence of the AS4/3501-6 moduli and α_{22} are depicted in Figure 2. All properties are nondimensionalized with their respective room temperature values shown in Table 1. Figures 1 illustrates the nonlinear variation of the various piezoceramic properties with temperature. The greatest nonlinearity occurs for p_3 , while the other properties exhibit a more gradual variation. For purposes of this study, all material properties not illustrated in Figures 1 and 2 are assumed to remain constant with temperature.

APPLICATIONS

This section presents results of numerical studies to demonstrate the effects of incorporating temperature dependent material properties. The problem examined consists of a 37.2 cm x 22.8 cm x 0.75 mm [0/±45]_s AS4/3501-6 carbon/epoxy plate with discrete PZT-5A piezoceramic patches attached on both the top and bottom surfaces. There are fifteen 6.0 cm x 6.0 cm x 0.13 mm piezoceramic patches uniformly attached to each surface as shown in Figure 3, which also depicts the finite element discretization for this problem. A total of eight discrete layers are used through the thickness of the plate (one layer for each ply of the composite and piezoceramic). The plate is simply supported along the two edges parallel to the y-axis and free on the two edges parallel to the x-axis. Linear thermal gradients of different values are applied through-the-thickness of the plate with the bottom surface ($z/h = -0.5$) fixed at 20°C for all cases and the upper surface ($z/h = 0.5$) varying from 45°C to 170°C. The values of the thermal gradient are selected to fall within the temperature range of the AS4/3501-6 properties (Fig. 2). The objective of the numerical study is to contrast the effects of incorporating temperature dependent material properties with corresponding results when material properties are assumed to remain temperature independent at the room temperature values shown in Table 1.

Thermal Deflections. A combined active/sensory configuration of the piezoceramic patches is used to study the thermally induced bending deflections and the corresponding sensory voltages in the plate. In this configuration, the piezoceramic patches on the upper surface of the plate are configured as sensors with free electric potentials, while 0 Volts are applied to all the patches on the bottom surface. All piezoceramic patches are grounded on the surface in contact with the carbon/epoxy

plate. The resulting thermally induced deflection at the center of the plate is shown in Figure 4 for different applied gradients. The deflections are nondimensionalized with respect to the total laminate thickness ($h=1.01$ mm). The figure shows that when material properties are assumed to be temperature independent, a linear variation in deflection is predicted. In contrast, a nonlinear variation in the deflection is observed when temperature dependence is incorporated into the analysis. Greater discrepancies between the two cases are observed as larger thermal gradients are applied.

Sensory Voltages. The corresponding sensory voltages generated by the central piezoceramic patch on the upper surface of the plate is shown in Figure 5. As in the case of the deflections, the assumption of constant material properties leads to a linear variation of the sensory voltages, while nonlinearities are introduced when temperature dependent material properties are modeled. Closer agreement is observed between the two cases than for the deflections. In actual smart structures applications, the measured sensory voltages would be used as input into a control algorithm to generate the necessary applied voltages to the actuators to minimize the thermal deflections.

Thermal Shape Control. A fully active configuration of the piezoceramic patches is used to study thermal shape control applications. In this configuration, all the piezoceramic patches are used as actuators to minimize the initial bending deformation. The same active voltages are applied to the inner surface of all the piezoceramic patches (i.e. the surface in contact with the carbon/epoxy plate), while the outer surface is grounded. The initial bending deformation to be minimized is shown in Figure 6 for the case in which the plate is subjected to a 100°C gradient with 0 Volts applied to the actuators. This deformation can be gradually eliminated through the application of increasing active voltages to the piezoceramic actuators. Figures 7 and 8 illustrate the reduction in bending achieved by applying active voltages of 72 V and 145 V, respectively. These results demonstrate the capability for thermal shape control using piezoceramic actuators.

Figure 9 depicts the active voltages applied to all the patches to minimize the deflection at the center of the plate for different applied gradients. Once again, a nonlinear variation is predicted by the temperature dependent material property case, while the constant material property case shows a linear variation that increasingly deviates as larger thermal gradients are applied. The increasing discrepancy in the active voltages required to minimize the initial deformation between the two cases corresponds to the same trend observed for the deflection at the center of the plate (Fig. 4). Since the temperature dependent case results in significantly larger deflections for higher temperatures, this in part justifies why larger active voltages are necessary to control the deflections.

Thermal Stresses. The stress fields associated with the plate in a fully active configuration are presented in this section. A continuous piezoceramic layer is used instead of discrete patches to reduce the need for a highly refined mesh in this study. The resulting normal stress (σ_{xx}) near the center of the plate ($x/a=0.5$, $y/b=0.4$, $z/h=0.8$) for different applied gradients is shown in Figure 10 for applied active voltages of 0 and 100 Volts. The stresses are nondimensionalized using a product of the corresponding longitudinal PZT-5A modulus, E_{11} , and the total laminate thickness, h . As in the previous cases, the assumption of constant material properties leads to a linear variation of the stresses with temperature, while nonlinearities are introduced when the temperature dependence in material properties is incorporated. Once again, the two cases show larger discrepancies as larger

thermal gradients are applied. The application of an active voltage of 100 V produces a corresponding reduction in normal stress from the 0 V case. The variation of the stress through-the-thickness near the center of the plate is illustrated in Figure 11 for the case in which the plate is subjected to a 150°C gradient with 100 V applied to the actuators. The results indicate that incorporating temperature dependent material properties produce generally higher stress levels in all plies of the plate.

One of the major advantages of using a layerwise approach is to improve the accuracy of out-of-plane shear stress predictions. Figure 12 shows the variation of the out-of-plane shear stress (σ_{xz}) near the free edge of the plate ($x/a=0.8$, $y/b=0.5$, $z/h=0.9$) for different applied gradients with active voltages of 0 and 100 V. The stresses are nondimensionalized using a product of the corresponding PZT-5A shear modulus, G_{13} , and the total laminate thickness, h . Once again, the use of temperature dependent material properties introduces a nonlinear variation in the stress with temperature, which increasingly deviates from the constant material case as higher applied gradients are applied. Application of active voltages of 100 V produces a decrease in the shear stress from the 0 V case. The variation of the stress through the thickness near the free edge of the plate with an applied gradient of 150°C and 100 V is shown in Figure 13. Closer agreement between the constant material property and temperature dependent material property case is observed for the shear stress.

SUMMARY

Layerwise mechanics were extended to account for the temperature dependence of the composite and piezoelectric material properties, which were incorporated as piecewise linear functions of temperature into the thermopiezoelectric constitutive relations. This formulation provides a unified capability to comprehensively model the coupled mechanical, electrical, and thermal behavior of active and sensory piezoelectric composite laminates. A finite element formulation was developed and implemented for a bilinear plate element. Numerical studies were conducted on a simply supported carbon/epoxy plate with attached piezoceramic patches subjected to thermal gradients. Results indicate that significant nonlinearities in the variation of displacement, sensory voltages, active voltages to minimize the centerline deflections, and stresses are introduced when temperature dependent material properties are incorporated into the analysis. This indicates the importance of including temperature dependent material properties in the analysis of thermal piezoelectric composite structures. Future experimental work is required in connection with the analytical developments to characterize the thermal behavior of piezoelectric composite structures.

REFERENCES

Chandrashekhara, K. and Kolli, M. (1995). Thermally Induced Vibration of Adaptive Doubly Curved Composite Shells with Piezoelectric Devices. *Proceedings of the 36th Structures, Structural Dynamics, and Materials Conference and Adaptive Structures Forum*. New Orleans, LA. April 10-13, 1995. 1628-1636.

Crawley, E.F (1994). Intelligent Structures for Aerospace: A Technology Overview and Assessment. *AIAA J.* **32:8**, 1689-1699.

Daniel, I.M. and Ishai, O. (1994). Engineering Mechanics of Composite Materials. Oxford University Press, New York.

Jonnalagadda, K.D., Blandford, G.E., and Tauchert, T.R. (1994). Piezothermoelastic Composite Plate Analysis Using First-Order Shear Deformation Theory. *Comput. Struct.* **51:1**, 79-89.

Lee, H.-J. and Saravanos, D.A. (1995). A Coupled Layerwise Analysis of the Thermopiezoelectric Response of Smart Composite Beams. *NASA TM 106889*.

Lee, H.-J. and Saravanos, D.A. (1996a). Coupled Layerwise Analysis of Thermopiezoelectric Composite Beams. *AIAA J.* **34:6**, 1231-1237.

Lee, H.-J. and Saravanos, D.A. (1996b). Layerwise Finite Elements for Smart Piezoelectric Composite Plates in Thermal Environments. *NASA TM 106990*.

Mindlin, R.D. (1974). Equations of High Frequency Vibrations of Thermopiezoelectric Crystal Plates. *Int. J. Solids Struct.* **10**, 625-632.

Rao, S.S. and Sunar, M. (1993). Analysis of Distributed Thermopiezoelectric Sensors and Actuators in Advanced Intelligent Structures. *AIAA J.* **31:7**, 1280-1286.

Rao, S.S. and Sunar, M. (1994). Piezoelectricity and Its Use in Disturbance Sensing and Control of Flexible Structures: A Survey. *Appl. Mech. Rev.* **47:4**, 113-123.

Robbins, D.H. and Reddy, J.N. (1991). Analysis of Piezoelectrically Actuated Beams Using a Layer-Wise Displacement Theory. *Comput. Struct.* **41:2**, 265-279.

Robbins, D.H. and Reddy, J.N. (1993). Modelling of Thick Composites Using a Layerwise Laminate Theory. *Int. J. Numer. Method Eng.* **36**, 655-677.

Tauchert, T.R. (1992). Piezothermoelastic Behavior of a Laminated Plate. *J. Thermal Stresses.* **15**, 25-37.

Tzou, H.S. and Howard, R.V. (1994). A Piezothermoelastic Thin Shell Theory Applied to Active Structures. *J. Vib. Acoust.* **116**, 295-302.

Tzou, H.S. and Ye, R. (1994). Piezothermoelasticity and Precision Control of Piezoelectric Systems: Theory and Finite Element Analysis. *J. Vib. Acoust.* **116**, 489-495.

TABLE 1: Material properties of piezoceramic (PZT-5A) and carbon/epoxy (AS4/3501-6) composite

	Piezoceramic	Carbon/Epoxy
Density (kg/m ³):		
ρ	7700.	1580.
Elastic Moduli (GPa):		
E_{11}	69.0	142.0
E_{22}	69.0	10.3
E_{33}	53.0	10.3
Poisson's Ratio:		
ν_{12}	0.31	0.27
ν_{23}	0.44	0.20
ν_{31}	0.38	0.02
Shear Moduli (GPa):		
G_{12}	23.3	7.2
G_{23}	21.1	4.29
G_{31}	21.1	7.2
Thermal Expansion Coefficient ($\mu\text{m/m } ^\circ\text{C}$):		
α_{11}	1.2	-0.9
α_{22}	1.2	27.0
Piezoelectric Charge Constant (pm/V) :		
d_{31}	-154.	----
Electric Permittivity (nf/m):		
ϵ_{33}	15.05	----
Pyroelectric Constant (mC/m ² $^\circ\text{C}$):		
P_3	-2.0	----
Reference Temperature, T_o , ($^\circ\text{C}$):	20.	20.
Curie Temperature, T_c , ($^\circ\text{C}$):	365.	----

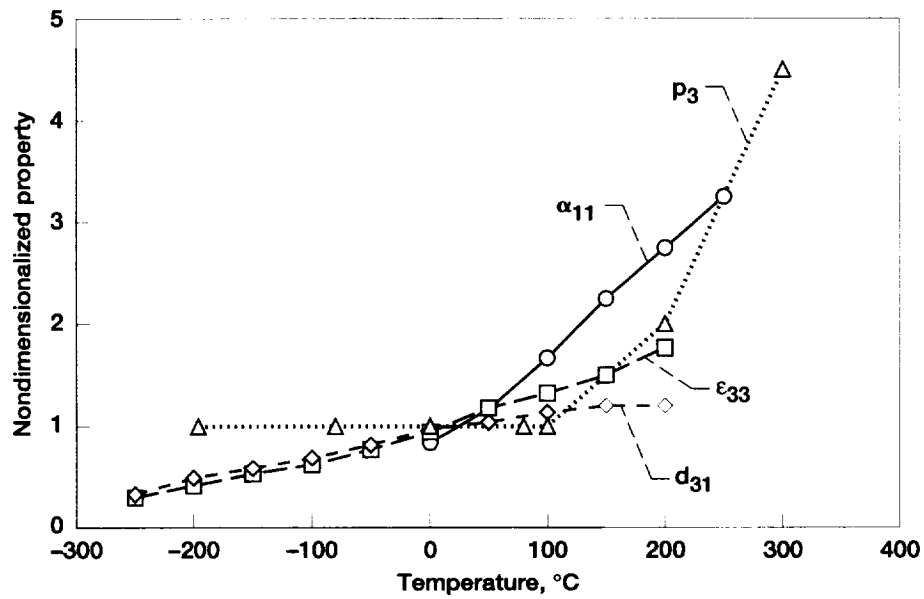


Figure 1.—Temperature dependence of PZT-5A properties. (d_{31} and ϵ_{33} data obtained from American Piezo Ceramics, Inc., Mackeyville, PA) (α_{11} and p_3 data obtained from Morgan Matroc, Inc., Bedford, OH).

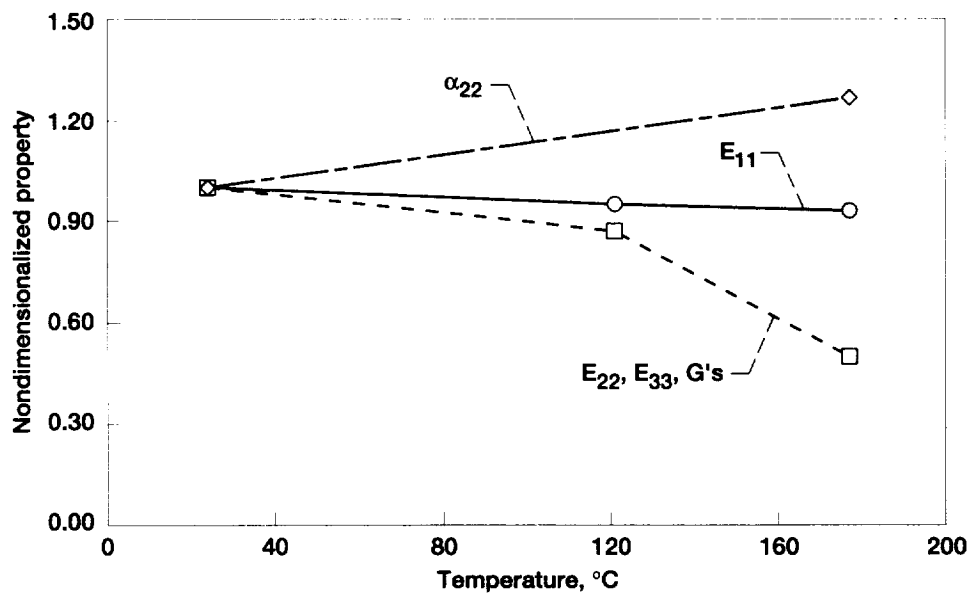


Figure 2.—Temperature dependence of AS4/3501-6 properties.

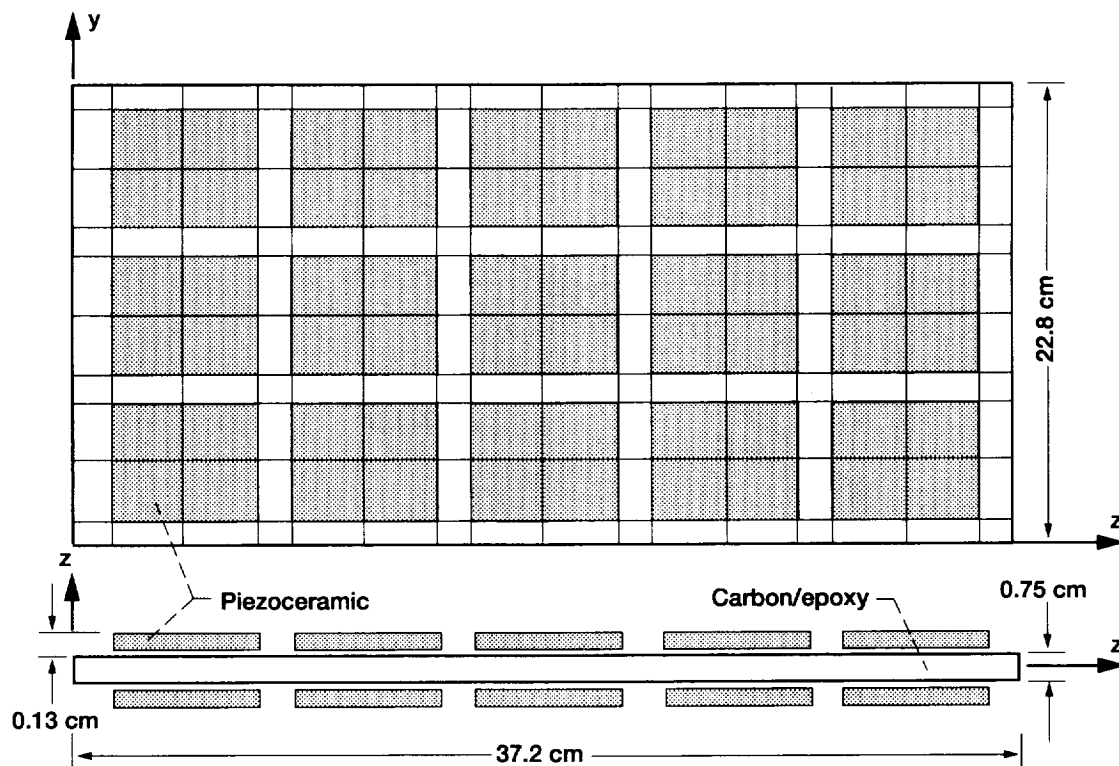


Figure 3.—Geometry and finite element mesh of AS4/3501-6 carbon/epoxy plate with attached PZT-5A piezoceramic patches.

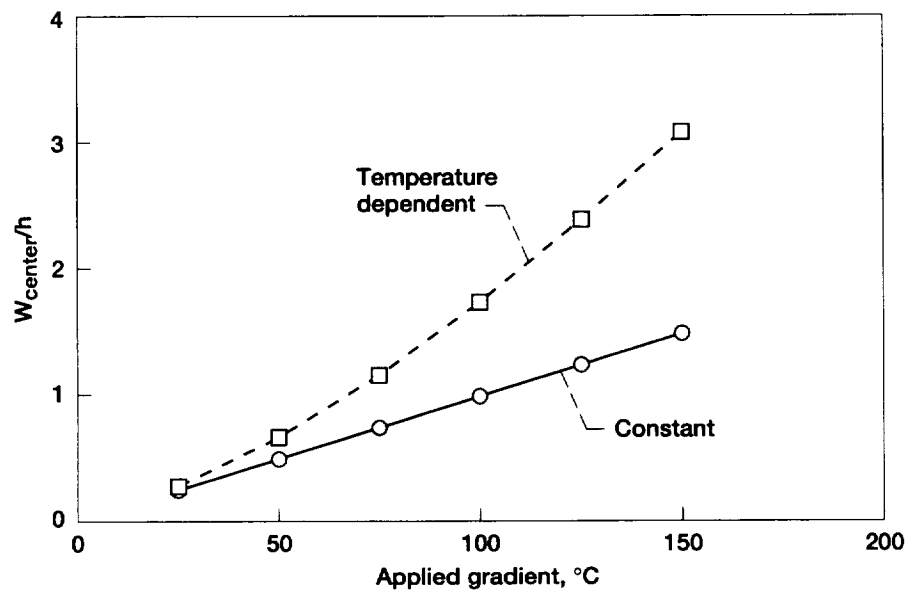


Figure 4.—Comparison of deflections at the center of the plate for different applied thermal gradients.

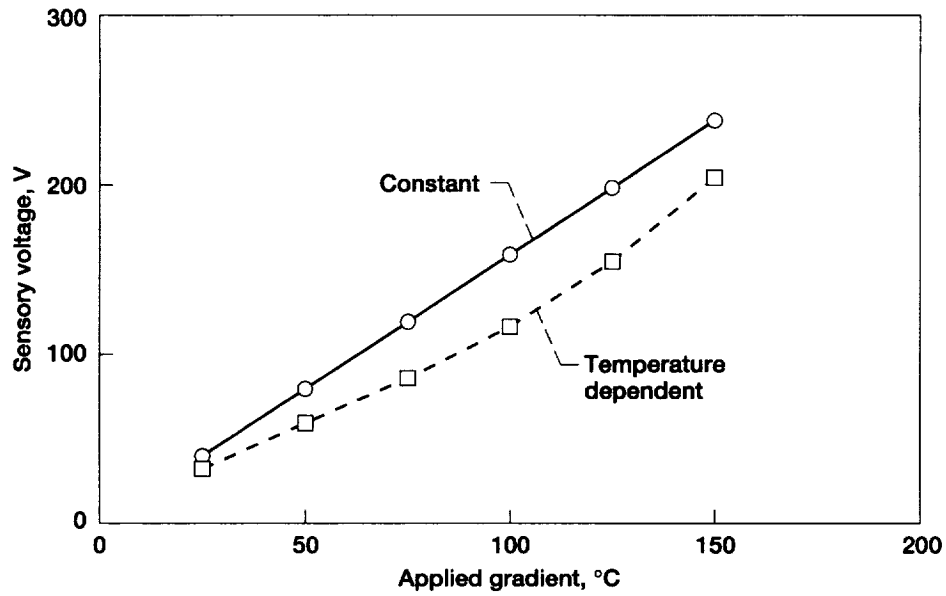


Figure 5.—Comparison of sensory voltages at the center of the plate for different applied thermal gradients.

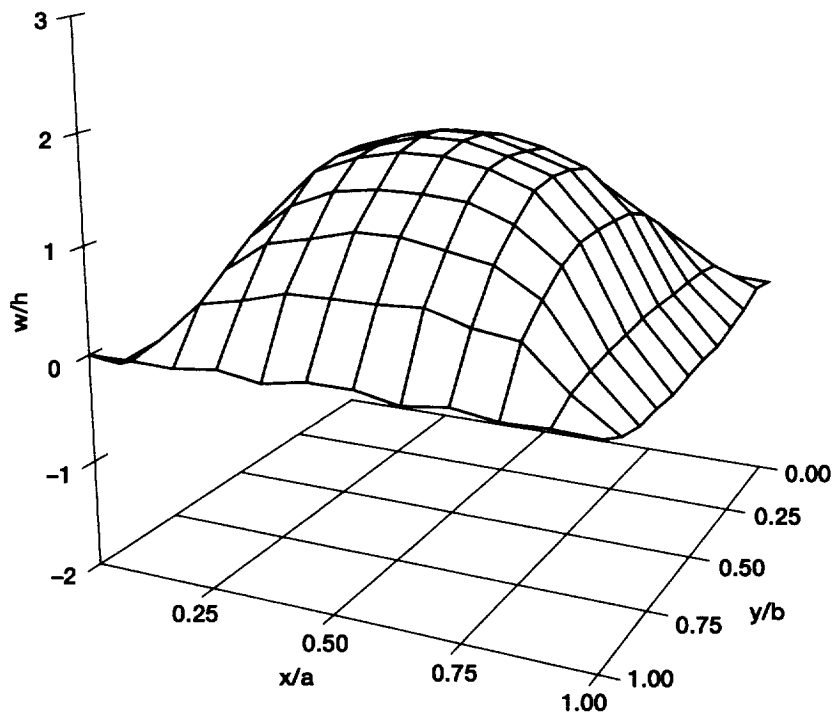


Figure 6.—Induced bending deflection under 100 °C gradient with actuators grounded.

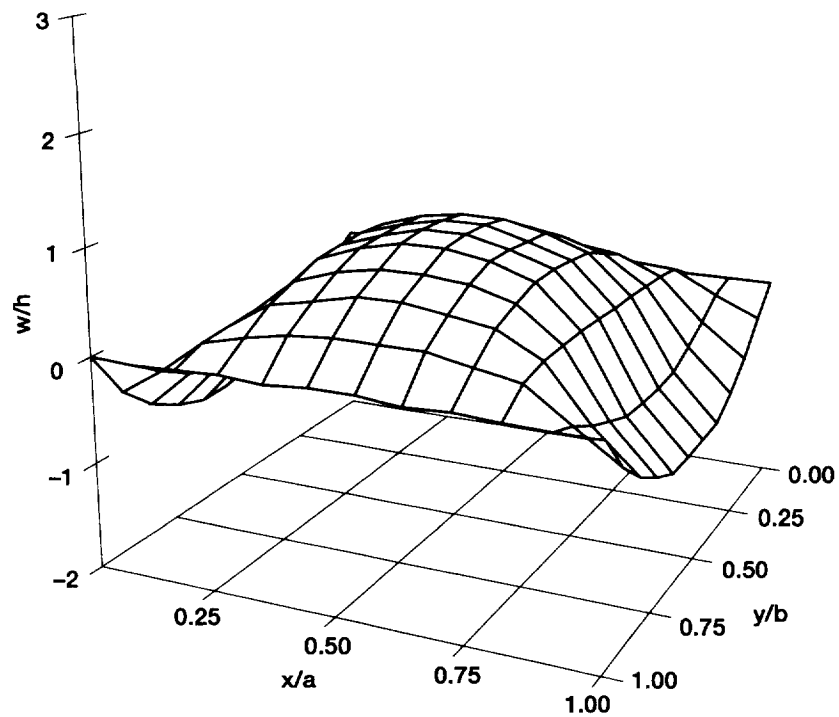


Figure 7.—Active shape control: 72 V applied to actuators.

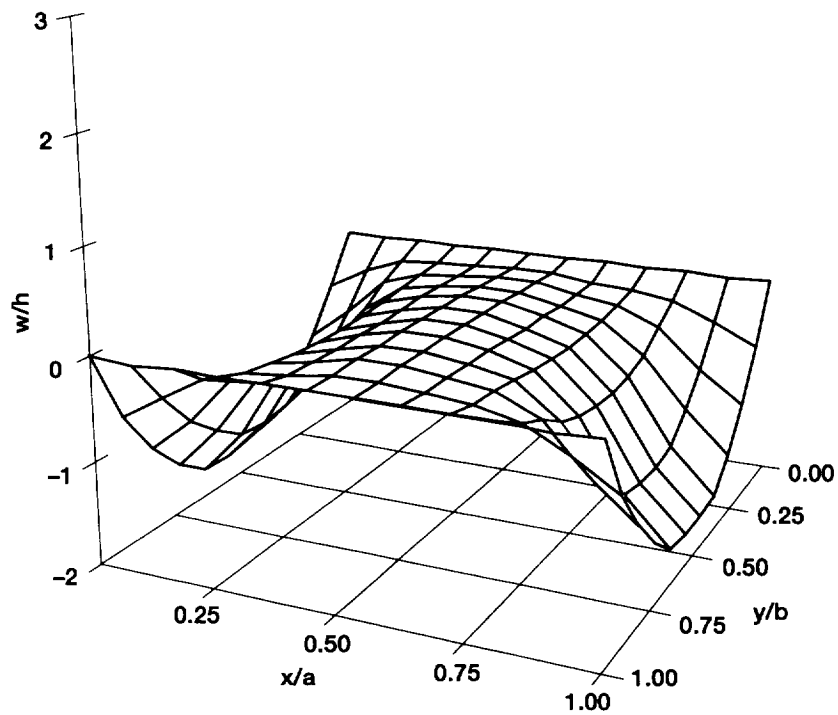


Figure 8.—Active shape control: 145 V applied to actuators.

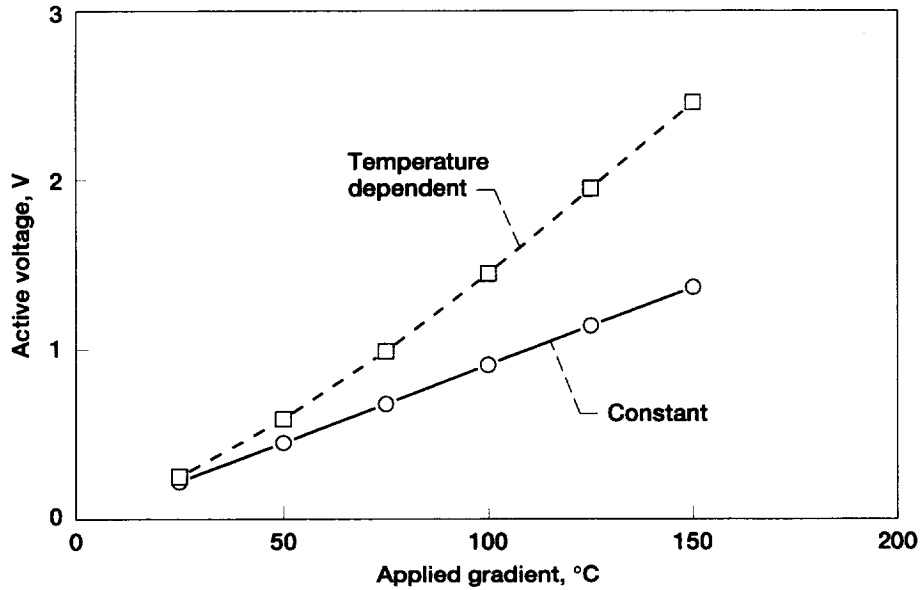


Figure 9.—Comparison of active voltages to minimize centerline deflections for different applied thermal gradients.

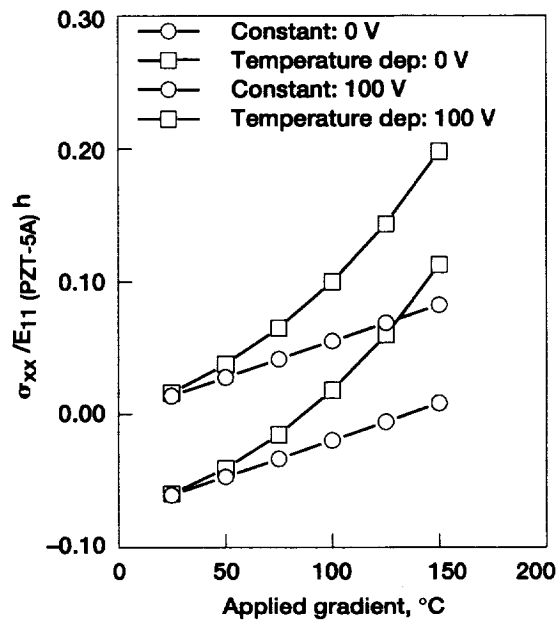


Figure 10.—Comparison of σ_{xx} at $(x/a = 0.5, y/b = 0.4, z/h = 0.8)$ for different applied thermal gradients.

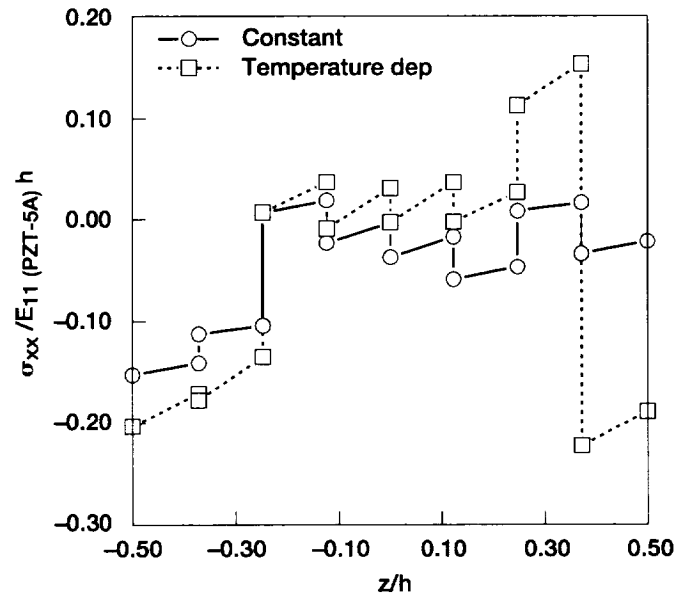


Figure 11.—Through the thickness variation of σ_{xx} under 150 °C gradient with 100 V applied to actuators.

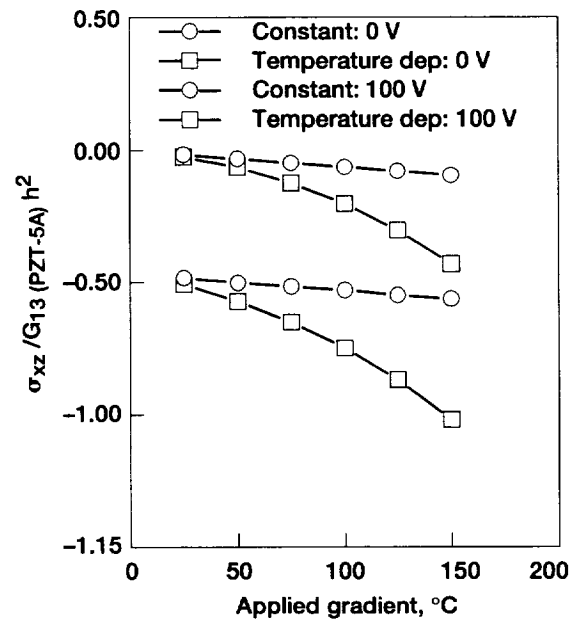


Figure 12.—Comparison of σ_{xz} at $(x/a = 0.9, y/b = 0.4, z/h = 0.9)$ for different applied thermal gradients.

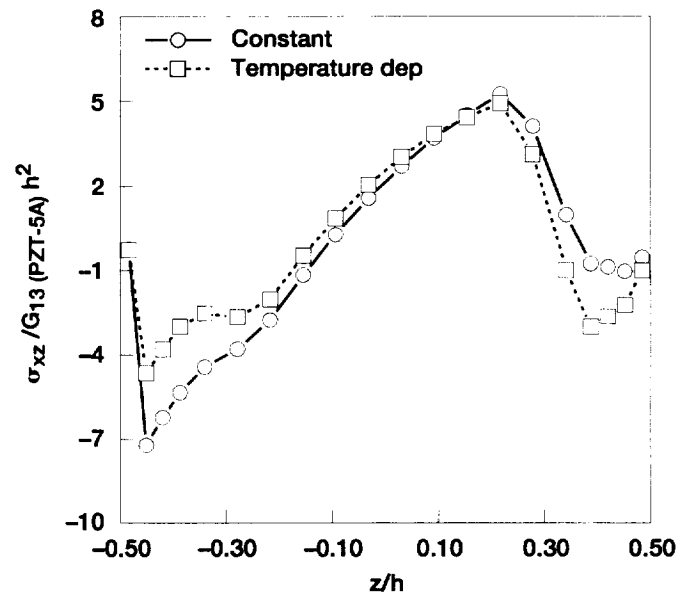


Figure 13.—Through the thickness variation of σ_{xz} under 150 °C gradient with 100 V applied to actuators.

REPORT DOCUMENTATION PAGE			Form Approved OMB No. 0704-0188	
Public reporting burden for this collection of information is estimated to average 1 hour per response, including the time for reviewing instructions, searching existing data sources, gathering and maintaining the data needed, and completing and reviewing the collection of information. Send comments regarding this burden estimate or any other aspect of this collection of information, including suggestions for reducing this burden, to Washington Headquarters Services, Directorate for Information Operations and Reports, 1215 Jefferson Davis Highway, Suite 1204, Arlington, VA 22202-4302, and to the Office of Management and Budget, Paperwork Reduction Project (0704-0188), Washington, DC 20503.				
1. AGENCY USE ONLY (Leave blank)		2. REPORT DATE November 1997		3. REPORT TYPE AND DATES COVERED Technical Memorandum
4. TITLE AND SUBTITLE The Effect of Temperature Dependent Material Nonlinearities on the Response of Piezoelectric Composite Plates			5. FUNDING NUMBERS WU-523-21-13-00	
6. AUTHOR(S) Ho-Jun Lee and Dimitris A. Saravanos				
7. PERFORMING ORGANIZATION NAME(S) AND ADDRESS(ES) National Aeronautics and Space Administration Lewis Research Center Cleveland, Ohio 44135-3191			8. PERFORMING ORGANIZATION REPORT NUMBER E-10952	
9. SPONSORING/MONITORING AGENCY NAME(S) AND ADDRESS(ES) National Aeronautics and Space Administration Washington, DC 20546-0001			10. SPONSORING/MONITORING AGENCY REPORT NUMBER NASA TM-97-206216	
11. SUPPLEMENTARY NOTES Ho-Jun Lee, NASA Lewis Research Center, and Dimitris A. Saravanos, Ohio Aerospace Institute, 22800 Cedar Point Road, Brook Park, Ohio 44142. Responsible person, Ho-Jun Lee, organization code 5910, (216) 433-3316.				
12a. DISTRIBUTION/AVAILABILITY STATEMENT Unclassified - Unlimited Subject Category: 24 This publication is available from the NASA Center for AeroSpace Information, (301) 621-0390.			12b. DISTRIBUTION CODE	
13. ABSTRACT (Maximum 200 words) Previously developed analytical formulations for piezoelectric composite plates are extended to account for the nonlinear effects of temperature on material properties. The temperature dependence of the composite and piezoelectric properties are represented at the material level through the thermopiezoelectric constitutive equations. In addition to capturing thermal effects from temperature dependent material properties, this formulation also accounts for thermal effects arising from: (1) coefficient of thermal expansion mismatch between the various composite and piezoelectric plies and (2) pyroelectric effects on the piezoelectric material. The constitutive equations are incorporated into a layerwise laminate theory to provide a unified representation of the coupled mechanical, electrical, and thermal behavior of smart structures. Corresponding finite element equations are derived and implemented for a bilinear plate element with the inherent capability to model both the active and sensory response of piezoelectric composite laminates. Numerical studies are conducted on a simply supported composite plate with attached piezoceramic patches under thermal gradients to investigate the nonlinear effects of material property temperature dependence on the displacements, sensory voltages, active voltages required to minimize thermal deflections, and the resultant stress states.				
14. SUBJECT TERMS Actuators; Composite materials; Finite element method; Piezoelectricity; Sensors; Smart structures; Temperature effects			15. NUMBER OF PAGES 22	
			16. PRICE CODE A03	
17. SECURITY CLASSIFICATION OF REPORT Unclassified	18. SECURITY CLASSIFICATION OF THIS PAGE Unclassified	19. SECURITY CLASSIFICATION OF ABSTRACT Unclassified	20. LIMITATION OF ABSTRACT	